

## Supporting Information

### **Multifunctional polymer-based nanocomposites for synergistic adsorption and photocatalytic degradation of mixed pollutants in water**

Jiao Wang,<sup>ab</sup> Nadia Licciardello,<sup>\*a</sup> Massimo Sgarzi,<sup>\*c</sup> and Gianaurelio Cuniberti<sup>\*a</sup>

<sup>a</sup> Institute for Materials Science, Max Bergmann Center of Biomaterials and Dresden Center for Nanoanalysis, TU Dresden, 01062, Dresden, Germany.

<sup>b</sup> Northwest Institute for Non-ferrous Metal Research, Xi'an, 710016, Shaanxi, P. R. China.

<sup>c</sup> Department of Molecular Sciences and Nanosystems, Ca' Foscari University of Venice, via Torino 155, 30172, Venezia Mestre, Italy

\* Corresponding authors: [nadia.licciardello@tu-dresden.de](mailto:nadia.licciardello@tu-dresden.de); [massimo.sgarzi@unive.it](mailto:massimo.sgarzi@unive.it); [gianaurelio.cuniberti@tu-dresden.de](mailto:gianaurelio.cuniberti@tu-dresden.de)

#### **Additional Experimental section**

##### ***Nanocomposites' adsorption capacity and photocatalytic activity towards BF***

In order to study the adsorption capacity of the nanocomposites towards BF, 23 mg of the nanocomposites were added into 50 mL of BF solution (1 mg/L, pH = 6) with stirring under dark conditions for 430 min (concentration of the nanocomposite: 460 mg/L). The pH 6 is the natural pH observed when a solution of BF (at the used concentration) is dissolved in water without the addition of an acid or a base. During the adsorption, samples were withdrawn at adsorption times of 5, 10, 20, 30, 40, 60, 80, 100, 120, 140, 160, 180, 190, 195, 200, 210, 220, 240, 260, 280, 310, 340, 400

and 430 min.

To evaluate both the adsorption capacity and the photocatalytic degradation ability of the nanocomposites towards BF in the conditions used in this study, 23 mg of the nanocomposites were added into 50 mL of BF solution (BF concentration: 1 mg/L, pH = 6, nanocomposites concentration: 460 mg/L) under stirring in dark conditions for 190 min to reach the adsorption-desorption equilibrium. During the adsorption, samples were withdrawn at adsorption times of 5, 10, 20, 30, 40, 60, 80, 100, 120, 140, 160, 180 and 190 min. After that, the remaining solution was placed under visible-light irradiation and stirring for 240 min. Samples were taken at 0 min (equivalent to 190 min in the former adsorption process, without irradiation) 5, 10, 20, 30, 50, 70, 90, 120, 150, 210 and 240 min of visible-light irradiation.

All the samples were centrifuged with an Eppendorf 5417 centrifuge (Hamburg, Germany) for 20 min at 20817 g and 20 °C to remove the suspended nanocomposites. The absorbance changes of the BF solutions were spectrophotometrically monitored at the BF absorption maximum (543 nm).

#### ***Nanocomposites' adsorption capacity and photocatalytic activity towards CIP***

To evaluate both the adsorption capacity and the photocatalytic degradation ability of the nanocomposites towards CIP, 23 mg of the nanocomposites were added into 50 mL of CIP solution (CIP concentration: 1 mg/L, pH = 4.3, nanocomposites concentration: 460 mg/L) under stirring and dark conditions for 100 min to reach the adsorption-desorption equilibrium. During the adsorption, samples were withdrawn at adsorption times of 5, 10, 20, 30, 40, 60, 80 and 100 min. After that, the solution was placed under visible-light irradiation and stirring for 240 min. During the visible-light irradiation, samples were taken at 0 min (equivalent to 100 min in the former adsorption process, without irradiation) 5, 10, 20, 30, 50, 70, 90, 120, 150, 180, 210 and 240 min after the visible-light irradiation started. All samples were centrifuged for 20 min at 20817 g and 20 °C to remove the suspended nanocomposites. The absorbance changes of CIP were spectrophotometrically monitored at the CIP

absorption maximum (277 nm).

## Additional results and discussion

### *Adsorption capacity and photocatalytic activity of the nanocomposites towards BF*

In order to study the photocatalytic degradation ability of the nanocomposites towards BF (1 mg/L), the adsorption capacity was first investigated. The experimental results shown in *Figure S1* show that, after 430 min, the adsorption percentage of BF was 87%.

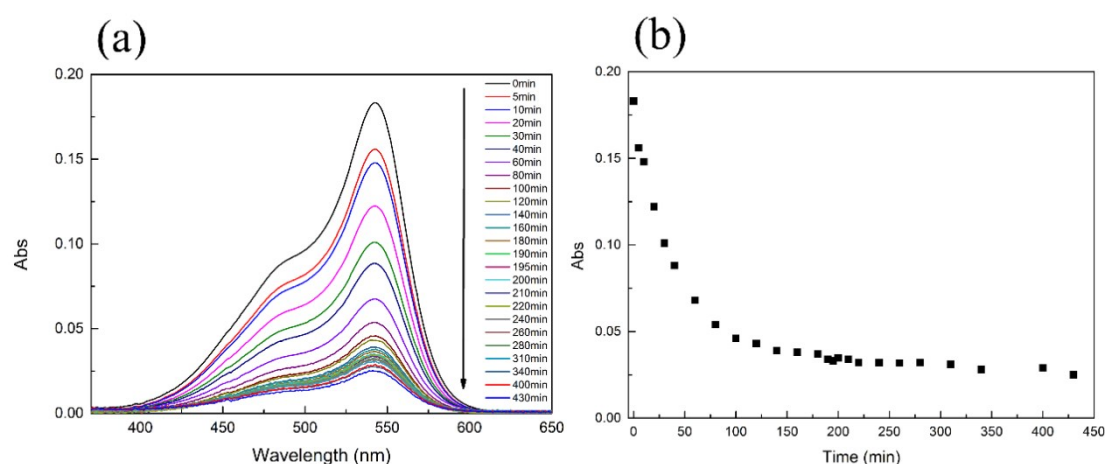


*Figure S1.* (a) Temporal variation of BF absorption spectrum and (b) adsorption kinetic curve of BF (1 mg/L, pH = 6) in the presence of the nanocomposites (460 mg/L) under dark conditions for 430 min.

Afterwards, the adsorption and visible-light photocatalytic degradation of BF by the nanocomposites were assessed (*Figure S2*). The nanocomposites were mixed with BF (1 mg/L) and stirred under dark conditions for 190 min, when an adsorption percentage of 81% was registered. Subsequently, the mixture was placed under visible-light irradiation for 240 min. After this time, only 8% of BF was apparently removed. Overall, 89% of BF was removed by the nanocomposites after 430 min of adsorption and subsequent photocatalytic degradation. Nevertheless, this value was similar to the one obtained when BF was only adsorbed by the nanocomposites (87%, *Figure S1*), indicating that the visible-light photocatalytic activity of the nanocomposites towards BF is negligible, and that the decrease of absorbance under visible-light irradiation has to be ascribed to the ongoing adsorption process.

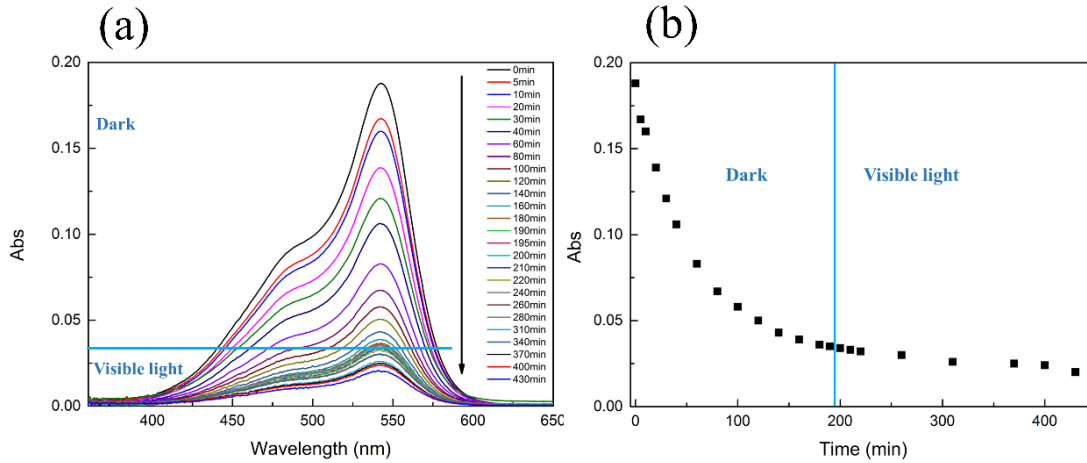


Figure S2. (a) Temporal variation of BF absorption spectrum and (b) kinetic curve of BF (1 mg/L, pH = 6) in the presence of the nanocomposites (460 mg/L) under 190 min dark conditions and subsequent 240 min of visible-light irradiation. The light blue line indicates the start of the visible-light irradiation process.

Pseudo-first-order (Equation [2]) and pseudo-second-order (Equation [3]) models were used to analyze the adsorption kinetics of the nanocomposites towards BF in Figure S1. The results are shown in Figure S3 and Table S1, which show that the kinetic data are better fitted with the pseudo-second-order model than with the pseudo-first-order one. The first piece of evidence for this conclusion is that the correlation coefficient value of the pseudo-second-order fitting ( $R^2 = 0.9958$ ) resulted higher than the one obtained with the pseudo-first-order one ( $R^2 = 0.8961$ ). Another piece of evidence is that the theoretical equilibrium adsorption capacity ( $q_e = 2.01$  mg/g) calculated using the pseudo-second-order model was closer to the experimental equilibrium adsorption capacity ( $q_{e,exp} = 1.91$  mg/g). The adsorption rate constant of the pseudo-second-order ( $k_2$ ) resulted  $0.0199 \text{ g} \cdot \text{mg}^{-1} \cdot \text{min}^{-1}$ . Besides, the adsorption kinetics of BF by the nanocomposites were better fitted with the pseudo-second-order model, indicating that the adsorption depends on both adsorbate and adsorbent and their interaction mainly controls this process<sup>1-3</sup>.

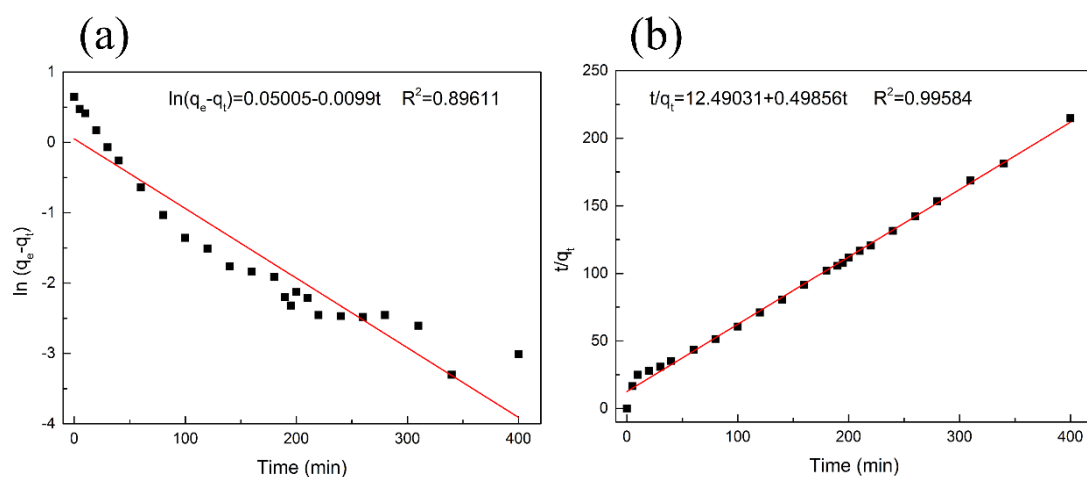


Figure S3. Adsorption kinetics of BF on the nanocomposites: (a) pseudo-first-order fitting and (b) pseudo-second-order fitting (initial concentration of BF: 1 mg/L, pH = 6, concentration of the nanocomposites: 460 mg/L).

Table S1. Model parameters of adsorption kinetics for BF adsorption by the nanocomposites under dark conditions for 430 min.

Pollutant	$q_{e,exp}$ ( $mg \cdot g^{-1}$ )	Pseudo-first-order model			Pseudo-second-order model		
		$q_e$ ( $mg \cdot g^{-1}$ )	$k_1$ ( $min^{-1}$ )	$R^2$	$q_e$ ( $mg \cdot g^{-1}$ )	$k_2$ ( $g \cdot mg^{-1} \cdot min^{-1}$ )	$R^2$
<b>BF</b>	1.91	1.05	0.0099	0.8961	2.01	0.0199	0.9958

### *Nanocomposites' adsorption capacity and photocatalytic activity towards CIP*

As reported in our former publication<sup>4</sup>, CIP (5 mg/L, pH = 3) could only be degraded by the nanocomposites through photocatalysis under visible-light irradiation, but could not be adsorbed by the nanocomposites. In order to determine the adsorption capacity and the photodegradation ability of the nanocomposites towards CIP at the initial concentration of 1 mg/L (pH = 4.3), adsorption and photodegradation experiments were performed. The nanocomposites were dispersed in a CIP solution with 1 mg/L concentration and placed under stirring and dark conditions for 100 min. The adsorption percentage was 21% after 40 min (Figure S4). This value is higher compared to the previous results obtained for a 5 mg/L CIP solution (2%)<sup>4</sup>: this can be

ascribed to a different ratio CIP/nanocomposites. The observed pH increase from 3 to 4.3 might also play a role in the adsorption capacity of CIP by the nanocomposites. Since the  $pK_a$  of methacrylate groups in the nanocomposites is 4.28, at  $pH = 4.3$  a higher number of carboxylate groups are deprotonated and can interact with CIP<sup>5</sup>. The adsorption experiment was prolonged for another additional 60 min, showing the same percentage decrease. The results in *Figure S4(b)* suggest that the adsorption-desorption equilibrium was reached after 40 min. After 100 min adsorption under dark conditions, the mixture of CIP and nanocomposites was irradiated with visible light (*Figure S4*, part on the right side or the bottom side in respect to the light blue line). The results show that the degradation efficiency of CIP by the nanocomposites was 88% after 240 min of visible-light irradiation.

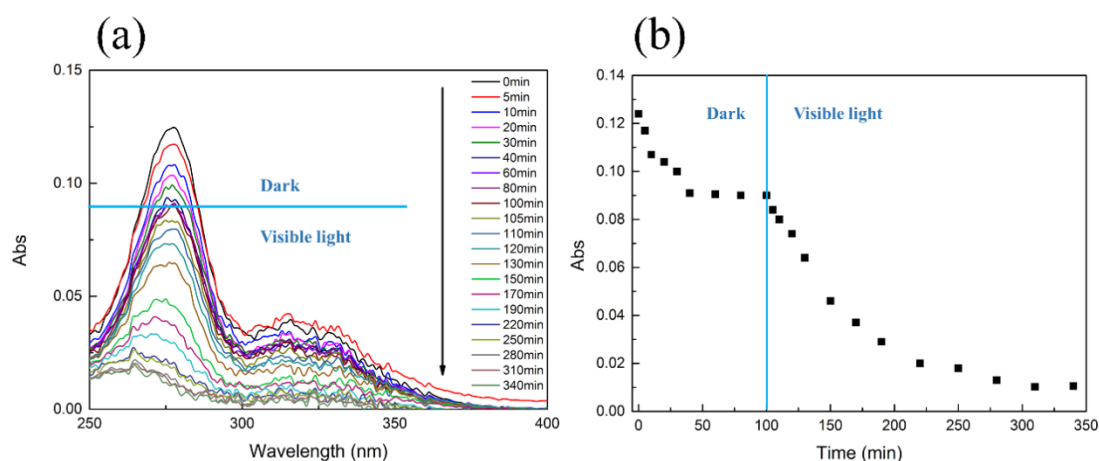


*Figure S4.* (a) Temporal variation of CIP absorption spectrum and (b) kinetic curve of CIP solution (1 mg/L,  $pH = 4.3$ ) in the presence of the nanocomposites (460 mg/L) under 100 min dark conditions and subsequent 240 min visible-light irradiation. The light blue line indicates the start of the visible-light irradiation step.

*Figure S5* and *Table S2* show that the adsorption kinetics data for CIP in the presence of the nanocomposites under dark conditions for 100 min are better fitted with the pseudo-second-order model than with the pseudo-first-order one. There are two pieces of evidence for this result. The first one is the correlation coefficient value of the pseudo-second-order fitting ( $R^2 = 0.9223$ ) which is higher than the one obtained for the pseudo-first-order one ( $R^2 = 0.6493$ ). The other one is that the theoretical

equilibrium adsorption capacity ( $q_e = 0.69 \text{ mg/g}$ ) calculated by the pseudo-second-order model is closer to the experimental equilibrium adsorption capacity ( $q_{e,\text{exp}} = 0.59 \text{ mg/g}$ ). The adsorption rate constant of the pseudo-second-order ( $k_2$ ) is  $0.1051 \text{ g}\cdot\text{mg}^{-1}\cdot\text{min}^{-1}$ . The adsorption kinetics for CIP in the presence of the nanocomposites was better fitted with the pseudo-second-order model, indicating that the adsorption of CIP on the nanocomposites depends both on the adsorbate and the adsorbent and that their interaction mainly controls the process<sup>1-3</sup>.

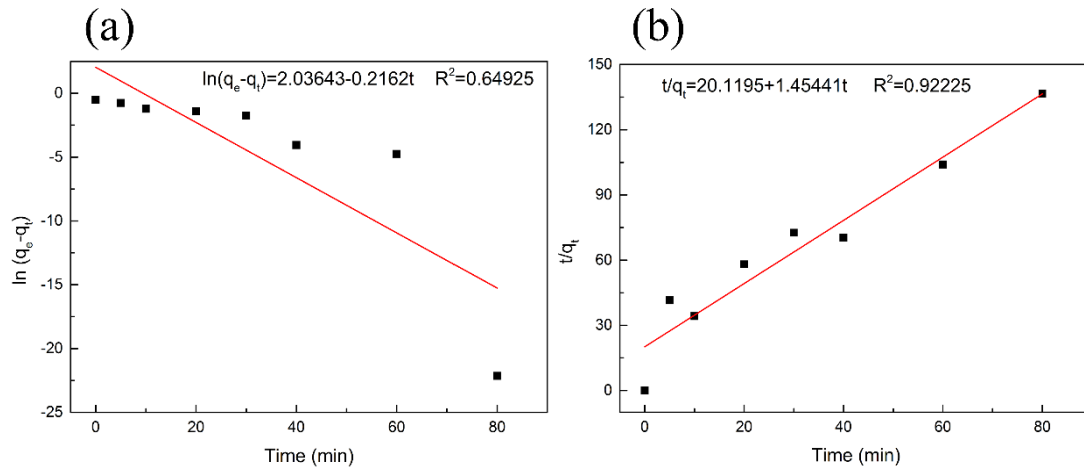


Figure S5. Adsorption kinetics of CIP on the nanocomposites under dark conditions for 100 min: (a) pseudo-first-order fitting and (b) pseudo-second-order fitting (initial concentration of CIP: 1 mg/L, pH = 4.3, concentration of the nanocomposites: 460 mg/L).

Furthermore, the photocatalytic degradation kinetics of CIP by means of the nanocomposites was analyzed by using equation [4]. The resulting degradation rate constant was  $4.31 \cdot 10^{-3} \text{ min}^{-1}$ .

Table S2. Model parameters of adsorption kinetics of CIP in the presence of the nanocomposites under dark conditions for 100 min.

Pollutant	$q_{e,\text{exp}}$ ( $\text{mg}\cdot\text{g}^{-1}$ )	Pseudo-first-order model			Pseudo-second-order model		
		$q_e$ ( $\text{mg}\cdot\text{g}^{-1}$ )	$k_1$ ( $\text{min}^{-1}$ )	$R^2$	$q_e$ ( $\text{mg}\cdot\text{g}^{-1}$ )	$k_2$ ( $\text{g}\cdot\text{mg}^{-1}\cdot\text{min}^{-1}$ )	$R^2$
CIP	0.59	7.66	0.2162	0.6493	0.69	0.1051	0.9223

In conclusion, on the contrary of BF, CIP (in a concentration of 1 mg/L, pH = 4.3) could be adsorbed and efficiently degraded (under visible-light irradiation) by the nanocomposites.

***Nanocomposites' adsorption capacity and photocatalytic activity towards a mixture of BF and CIP***

***Mixture 1:***

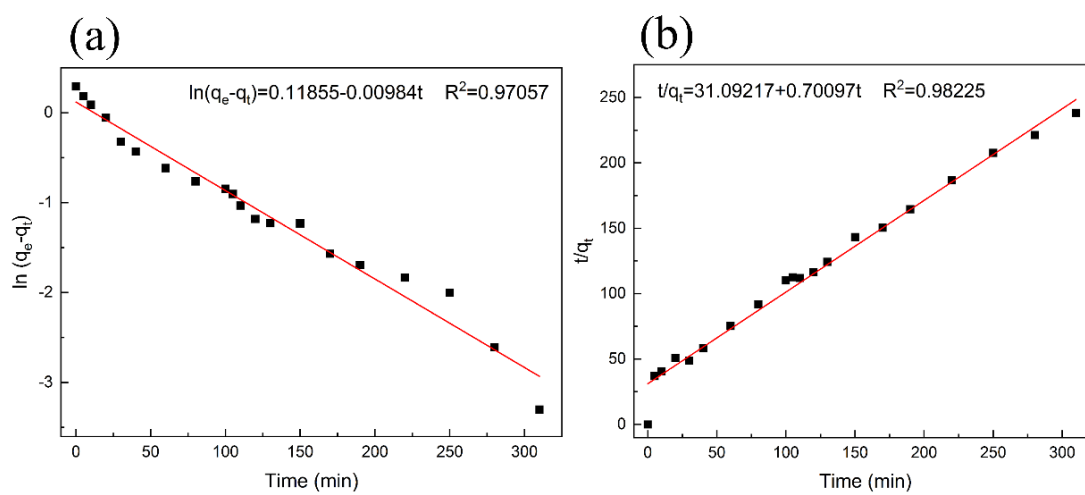


Figure S6. Adsorption kinetics fitting at 543 nm of BF in the presence of the nanocomposites for 340 min (the first 100 minutes in the dark and the second 240 minutes under visible-light irradiation, experiment Mixture 1): (a) pseudo-first-order fitting and (b) pseudo-second-order fitting.

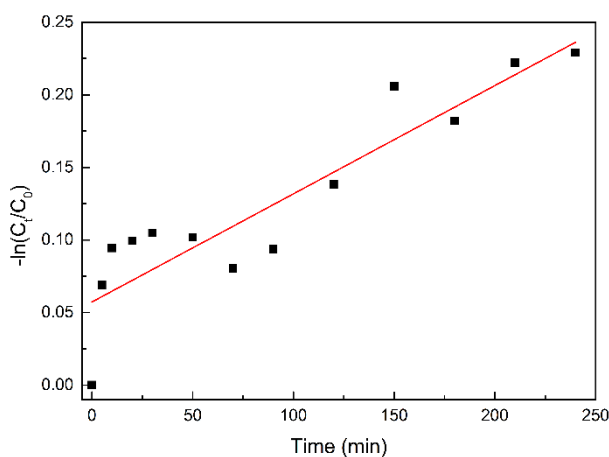


Figure S7. Pseudo-first-order kinetic fitting at 277 nm of CIP in the presence of the nanocomposites under visible-light irradiation for 240 min (0 min in Figure S7 is the 100 min in Figure 1 and is the

beginning of the photocatalytic experiment under visible-light irradiation). These are the results for the experiment Mixture 1.

**Mixture 2:**

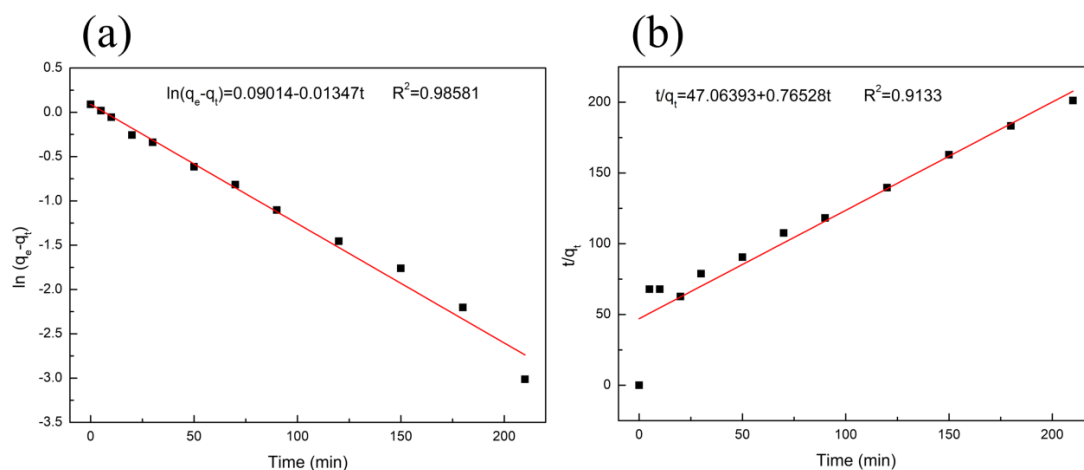


Figure S8. Adsorption kinetics fitting at 543 nm of BF in the presence of the nanocomposites over the 240 min of stage 3: (a) pseudo-first-order fitting and (b) pseudo-second-order fitting (0 min in Figure S8 corresponds to 290 min in Figure 2 and is the beginning of photocatalytic experiment under visible-light irradiation).

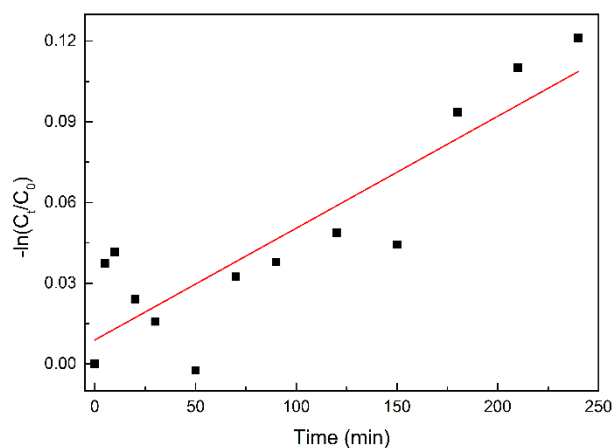


Figure S9. Pseudo-first-order kinetic fitting at 277 nm of CIP in the presence of the nanocomposites under visible-light irradiation over the 240 min of stage 3 (0 min in Figure S9 corresponds to 290 min in Figure 2 and is the beginning of photocatalytic experiment under visible-light irradiation).

### Mixture 3:

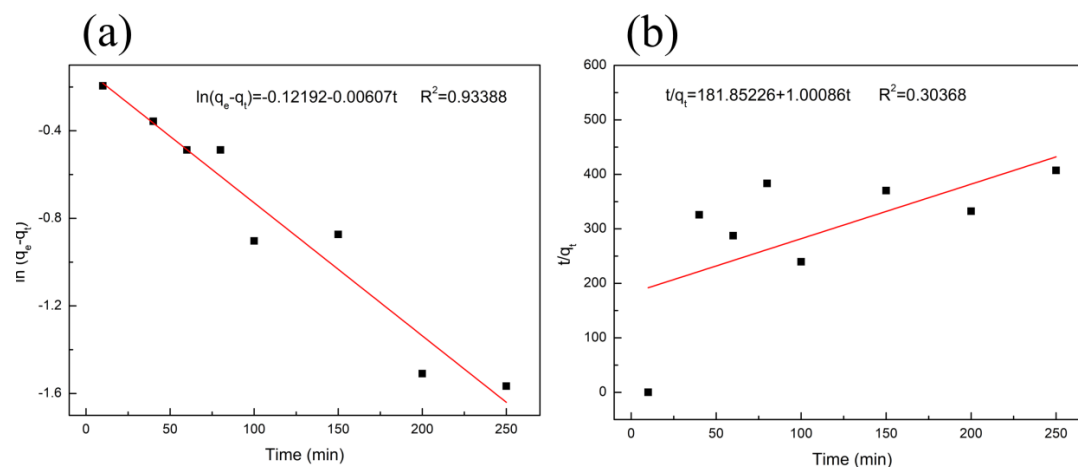


Figure S10. Adsorption kinetics fitting at 543 nm of BF by the nanocomposites for 300 min: (a) pseudo-first-order fitting and (b) pseudo-second-order fitting (0 min in Figure S10 corresponds to 340 min in Figure 3 and is the beginning of the adsorption experiment towards BF under visible-light irradiation).

### References

1. Yan, H. *et al.* Sorption of methylene blue by carboxymethyl cellulose and reuse process in a secondary sorption. *Colloids and Surfaces A: Physicochemical and Engineering Aspects* **380**, 143–151 (2011).
2. Iram, M., Guo, C., Guan, Y., Ishfaq, A. & Liu, H. Adsorption and magnetic removal of neutral red dye from aqueous solution using  $\text{Fe}_3\text{O}_4$  hollow nanospheres. *Journal of Hazardous Materials* **181**, 1039–1050 (2010).
3. Módenes, A. N. *et al.* Adsorption of direct of yellow ARLE dye by activated carbon of shell of coconut palm: Diffusional effects on kinetics and equilibrium states. *International Journal Bioautomation* **19**, 187–206 (2015).
4. Wang, J. *et al.* Reusable and Antibacterial Polymer-Based Nanocomposites for the Adsorption of Dyes and the Visible-Light-Driven Photocatalytic Degradation of Antibiotics. *Global Challenges* **6**, 2200076 (2022).

5. Wang, J., Zhang, W., Qian, Y., Deng, B. & Tian, W. pH, temperature, and magnetic triple-responsive polymer porous microspheres for tunable adsorption. *Macromolecular Materials and Engineering* **301**, 1132–1141 (2016).